

Electrochemical Fabrication of Nano Manganese Oxide Modified Electrode for the Detection of H₂O₂

Soundappan Thiagarajan, Tsung Hsuan Tsai, Shen-Ming Chen*

Electroanalysis and Bioelectrochemistry Lab, Department of Chemical Engineering and Biotechnology, National Taipei University of Technology, No.1, Section 3, Chung-Hsiao East Road, Taipei 106, Taiwan (ROC).

*E-mail: smchen78@ms15.hinet.net

Received: 1 May 2011 / Accepted: 25 May 2011 / Published: 1 June 2011

Electrochemical deposition of nano manganese oxide materials on indium tin oxide coated glass electrode (ITO) has been carried out using cyclic voltammetry. The surface morphology of the electrodeposited manganese oxide materials was examined using atomic force microscopy and the electrodeposited manganese oxide materials have been found as particle shaped in the average size range of 21 to 40 nm. Electrodeposited nano manganese materials were examined using X-ray diffraction analysis (XRD) and identified as in the different phases (MnO, MnO₂ and Mn₃O₄). The nano manganese oxide modified ITO electrode successfully shows the electrochemical oxidation current signals for the detection of H₂O₂ in pH 7.0 PBS. The sensitivity and detection limit for the H₂O₂ at the proposed electrode was found as 7.51 $\mu\text{A mM}^{-1}$ and 0.02 mM. Also, it shows acceptable linear range for the detection H₂O₂ in real samples.

Keywords: Nano manganese oxide, electrochemical deposition, indium tin oxide coated glass electrode, cyclic voltammetry, H₂O₂.

1. INTRODUCTION

Fabrication of metal and metal oxide nanostructures is found to be emerging area in the field of nanoscience and nanotechnology. Various methods have been employed for the fabrication of these metal oxide nanostructures. Here, the electrochemical fabrication of metal oxide nanostructures is found as promising aspect in the field of electrochemical science. Few examples were; electrochemical route for the synthesis of new nanostructure magnetic mixed oxides of Mn, Zn, and Fe from an acidic chloride and nitrate medium [1, 2], electrochemical deposition of bi-metallic nanostructures [3],

synthesis of nanocrystalline metal oxides using electrochemical deposition under the oxidizing conditions [4], films of MnO₂ nanoparticles and H₂O₂ for the electrochemical catalysis of styrene [5], Au nanoparticles–manganese oxide nanoparticles as binary catalysts for the electrocatalytic reduction of oxygen [6], synthesis and characterization of manganese oxide and hybrid nanocomposite thin films [7, 8], Au nanoparticles–MnO_x nanoparticles as binary catalysts on the electrochemical reduction of molecular oxygen [9], carbon-supported manganese oxide nanoparticles as electro catalysts for the oxygen reduction reaction (ORR) in alkaline medium [10], nano-manganese oxide for reduction of oxygen [11] and cyclic voltammetrically prepared copper-decorated MnO₂ for ORR reaction [12] were reported.

Further the manganese oxide nanomaterials modifications have wide potential applications. The manganese oxide nanocomposites widely applied in the fabrication of super capacitors. For example, graphene oxide MnO₂ nanocomposites [13], redox exchange induced manganese oxide embedded polypyrrole nanocomposites [14], construction of composite electrodes comprising manganese dioxide nanoparticles distributed in polyaniline–poly(4-styrene sulfonic acid-co-maleic acid) [15] and MnO₂ nanoparticles enrichment in poly(3,4-ethylenedioxythiophene) nanowires for electrochemical energy storage [16] were reported. Not only limited to this, manganese oxide nanocomposites also used for various types of electrocatalytic applications.

For example, manganese oxide nanorods modified electrodes for the enhanced water electrolysis [17], electrocatalytic oxidation of methanol at MnOOH Nanorods modified Pt electrodes [18], cholesterol biosensor based on MWCNTs-MnO₂ nanoparticles using cyclic voltammetry [19] and MnO₂-based nanostructures as catalysts for electrochemical oxygen reduction in alkaline media [20] were reported.

Hydrogen peroxide (H₂O₂) known as powerful oxidizer, antiseptic and anti bacterial agent have potential role in cleaning, sterilizing processes and in organic synthesis reactions. H₂O₂ directly affects the biological systems. Therefore, detection and determination of H₂O₂ is an important criterion in electroanalytical chemistry [21, 22]. H₂O₂ can be detected using various methods such like spectrophotometric [23], titrimetric [24], fluorescence and phosphorescence [25-26]. Among these methods, electrochemical analysis also found to be suitable for the detection and determination of H₂O₂. Different types of metal oxide materials such like, manganese oxide [27], iron oxide [28] cobalt oxide [29] nickel oxide [30], zirconium oxide [31] and tungsten oxide [32] were utilized for the fabrication H₂O₂ sensor. Also, gold nanoparticles mediated assembly of manganese oxide nanoparticles [33], nafion and manganese oxide microsphere modified electrodes [34] for the amperometric detection and direct electrocatalytic oxidation of H₂O₂ were also reported.

Based on the previous discussions and considering the potential importance of the manganese oxide nanomaterials, here we have attempted to fabricate nano manganese oxide modified indium tin oxide coated glass electrode (ITO) for the electrocatalytic oxidation of H₂O₂. We have employed cyclic voltammetry for the electrochemical fabrication of manganese oxide nanomaterials. Further the nanomaterials have been characterized using atomic force microscopy (AFM) and X-ray diffraction analysis (XRD). The electrochemical characteristics of the manganese nanomaterials have been confirmed by using electrochemical impedance analysis (EIS). The potential application of these nanomaterials was confirmed by detecting the H₂O₂ in lab and real samples.

2. MATERIALS AND METHODS

2.1. Reagents

Manganese (II) acetate was purchased from Sigma-Aldrich (USA). All other chemicals (Merck) used were of analytical grade (99 %). H_2O_2 (30 %) was purchased from Wako pure chemicals Ltd, Japan). A phosphate buffer solution (PBS) of pH 7.0 was prepared using Na_2HPO_4 (0.05 mol l^{-1}) and NaH_2PO_4 (0.05 mol l^{-1}). Pure nitrogen was passed through all the experimental solutions. Double distilled deionized water was used to prepare all the solutions. For the real sample analysis, antiseptic solution containing H_2O_2 was purchased from local drug store.

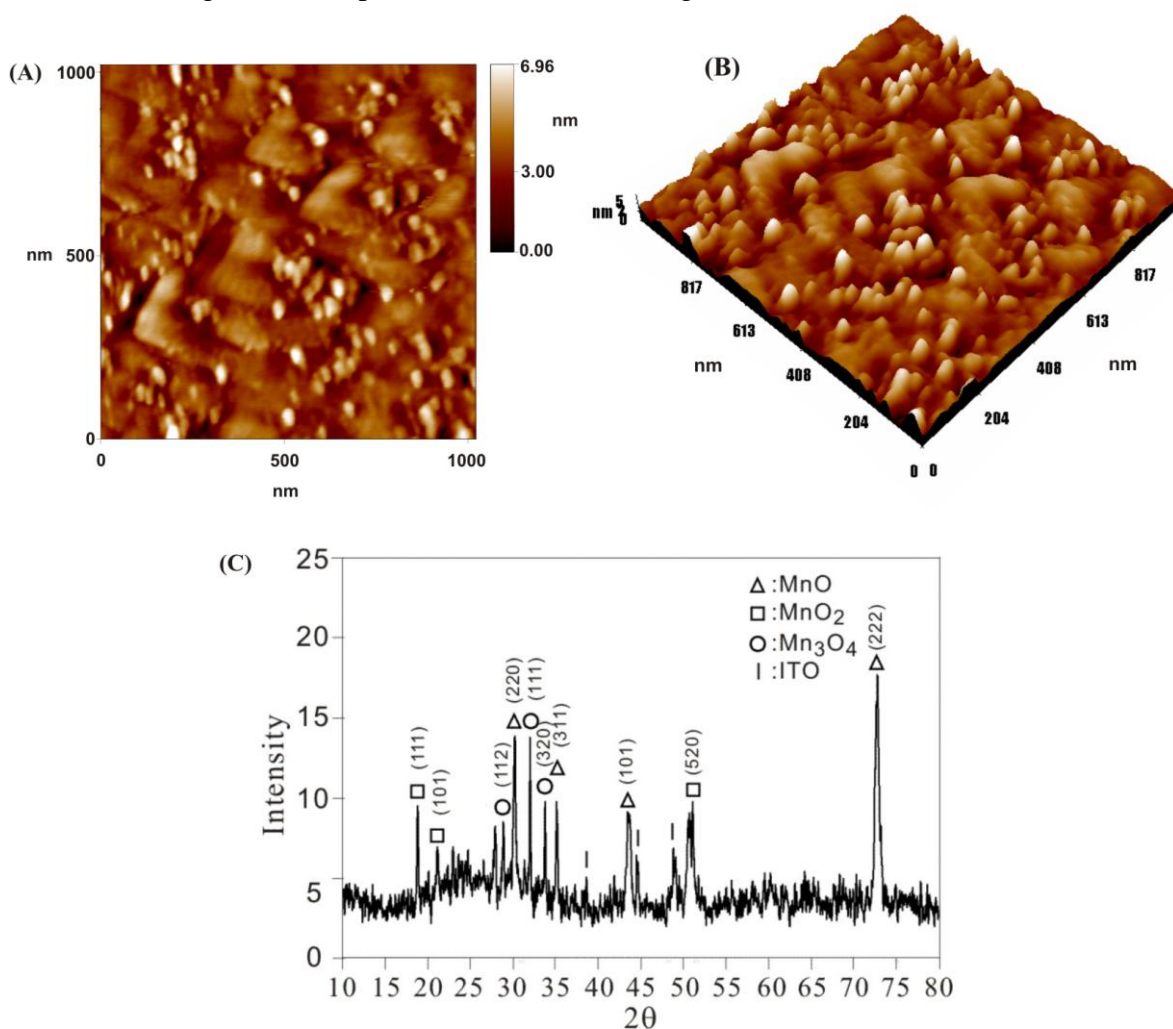


Figure 1. AFM images of (A) two dimensional and (B) three dimensional view of electrodeposited nano manganese oxide on ITO. (C) XRD pattern of nano manganese oxide electrodeposited on ITO.

2.2. Apparatus

All electrochemical experiments were performed using CHI 410a potentiostat (CH Instruments, USA). For the entire electrochemical analysis indium tin oxide coated glass electrodes (ITO) was used.

A conventional three-electrode system which consists of bare or nano manganese oxide layer electrochemical deposited ITO glass electrode as working electrode, an Ag/AgCl (saturated KCl) as a reference and platinum wire as counter electrode were used. The AFM images were recorded with multimode scanning probe microscope (Being Nano-Instruments CSPM-4000, China). The XRD experiment was done using XPERT-PRO (PANalytical B.V., The Netherlands). Electrochemical impedance studies (EIS) were performed using ZAHNER impedance analyzer (Germany).

2.3. Fabrication of nano Manganese Oxide on ITO

Indium tin oxide coated glass electrodes (ITO) have been immersed in deionized distilled water and kept for ultra sonication for one hour. Further the electrodes were immersed in Triton-X 100 surfactant solution for 30 minutes. After this process, the ITO electrodes washed thoroughly with deionized distilled water and used for the electrochemical deposition process. Here the cyclic voltammetry has been employed for the electrochemical deposition process. Pretreated ITO electrode has been immersed in the 0.1 M Na₂SO₄ solution containing 0.1 M manganese acetate solution and the potential has been fixed of 0 to 0.4 V at the scan rate of 20 mV/s for three cycles and the manganese oxide materials were directly deposited on the ITO electrode surface (Figure-2 (A)). Finally the manganese oxide materials modified ITO was rinsed with deionized water and employed for the electrochemical analysis.

3. RESULTS AND DISCUSSION

3.1. Characterization of nano manganese oxide materials modified ITO

Manganese oxide modified ITO was employed for the AFM analysis. Fig-1(A) and (B) show the two and three dimensional view of electrodeposited manganese oxide on ITO. Here the scan area was 1021 × 1021 nm. Here AFM tapping mode was applied for the surface morphological process. From the Fig-1(A) and (B), we can see the existence of electrodeposited manganese oxides in the particles shape within the average size range of 21 to 40 nm. Here manganese oxide particles were unevenly deposited on the ITO glass electrode surface. The roughness average for these nano particles deposited surface was found as 0.78 nm. The surface skewness (Rsk) and kurtosis (Rku) were known for the measurement of symmetry variation of the surface and the unevenness or sharpness of the surface. Here for this nano surface the surface skewness value found as 0.142 and the surface kurtosis (Rku) was 3.63. All these values are averages taken from the several scan process of the same surface. Based on the above discussed results we can able to conclude the electrodeposited nano manganese oxide particles on the ITO.

In the next step XRD has been employed for the further detailed analysis. Fig. 1(C) represents the X-ray diffraction pattern for the electrodeposited nano manganese oxide particles modified ITO. Here the electrodeposited nano manganese oxide particles were identified as a mixture of different phases such like MnO, MnO₂ and Mn₃O₄. In the Fig 1(C) we can notice the MnO diffraction patterns ((Δ) 220, 311, 101), MnO₂ diffraction patterns (□) 111, 101, 520) and Mn₃O₄ (O) 112, 111, 320) and

the remaining diffraction patterns (I) belongs to ITO [35-38]. Based on this XRD result, we assume that the nano manganese oxides were electrodeposited as a mixture in the different phases, respectively.

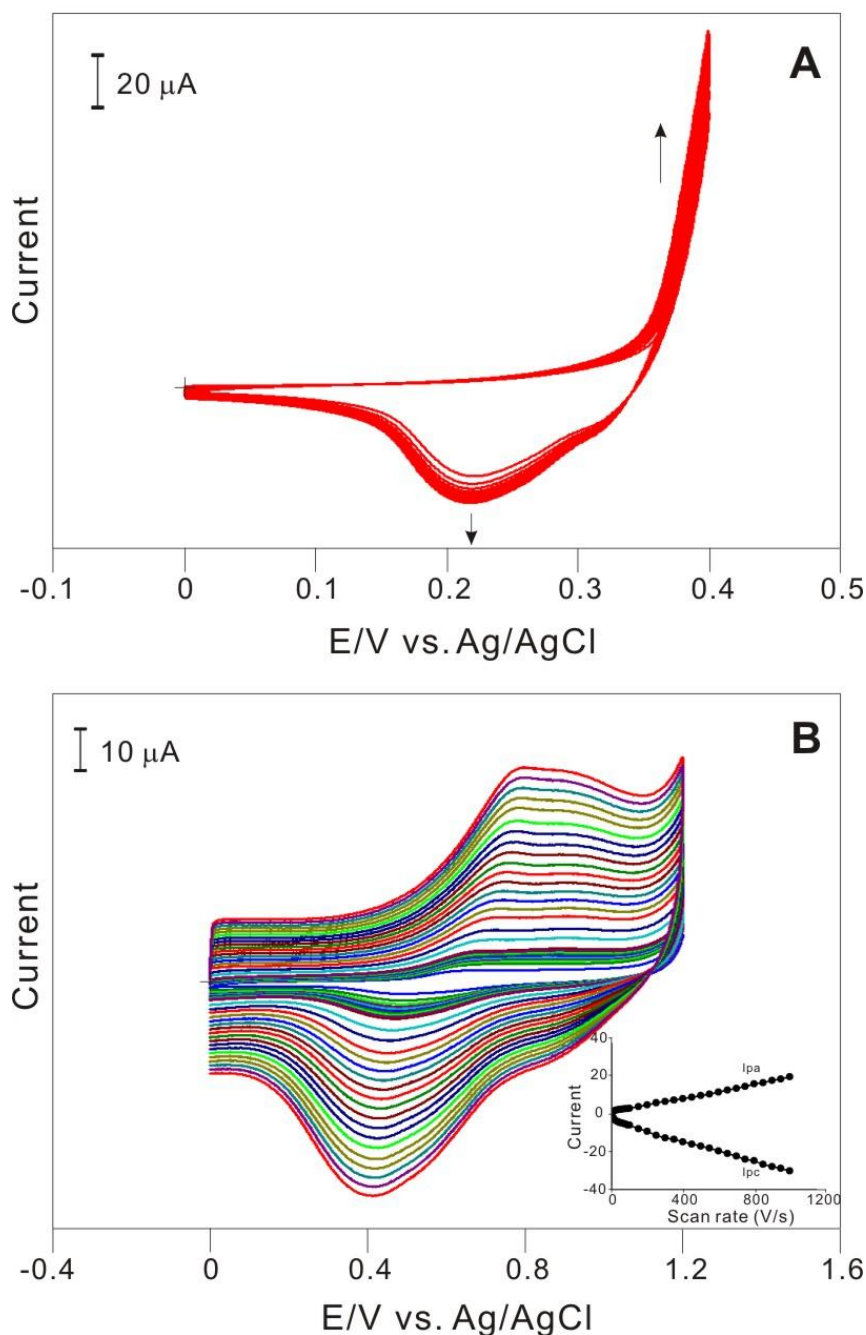


Figure 2. (A) Consecutive cyclic voltammograms (CV) of manganese oxide hybrid materials electrochemical deposition process on ITO using 0.1 M Na_2SO_4 (10 ml) containing 0.1 M $\text{Mn}(\text{CH}_3\text{COO})_2$ in the potential range of 0 to 0.4 V (scan rate: 20 mV/s) for 3 three cycles. (B) Different scan rate studies of manganese oxide hybrid materials modified ITO in pH 7.0 PBS. Scan rate in the range of 0.01 to 1 V/s. Inset shows the plots of anodic and cathodic peak currents vs. scan rate.

3.2. Electrochemical activities of the nano manganese oxide hybrid materials modified ITO

Fig. 2(A) shows the continuous cyclic voltammograms of nano manganese oxide electrodeposition process on ITO. Here the initial scan takes place at 0 V and ends at 0.4 V at the scan rate of 20 mV/s for three cycles. At the beginning, scan process run with sharp increase in the anodic peak (oxidation) at the 0.4 V and ends with the broad cathodic peak (at 0.21 V).

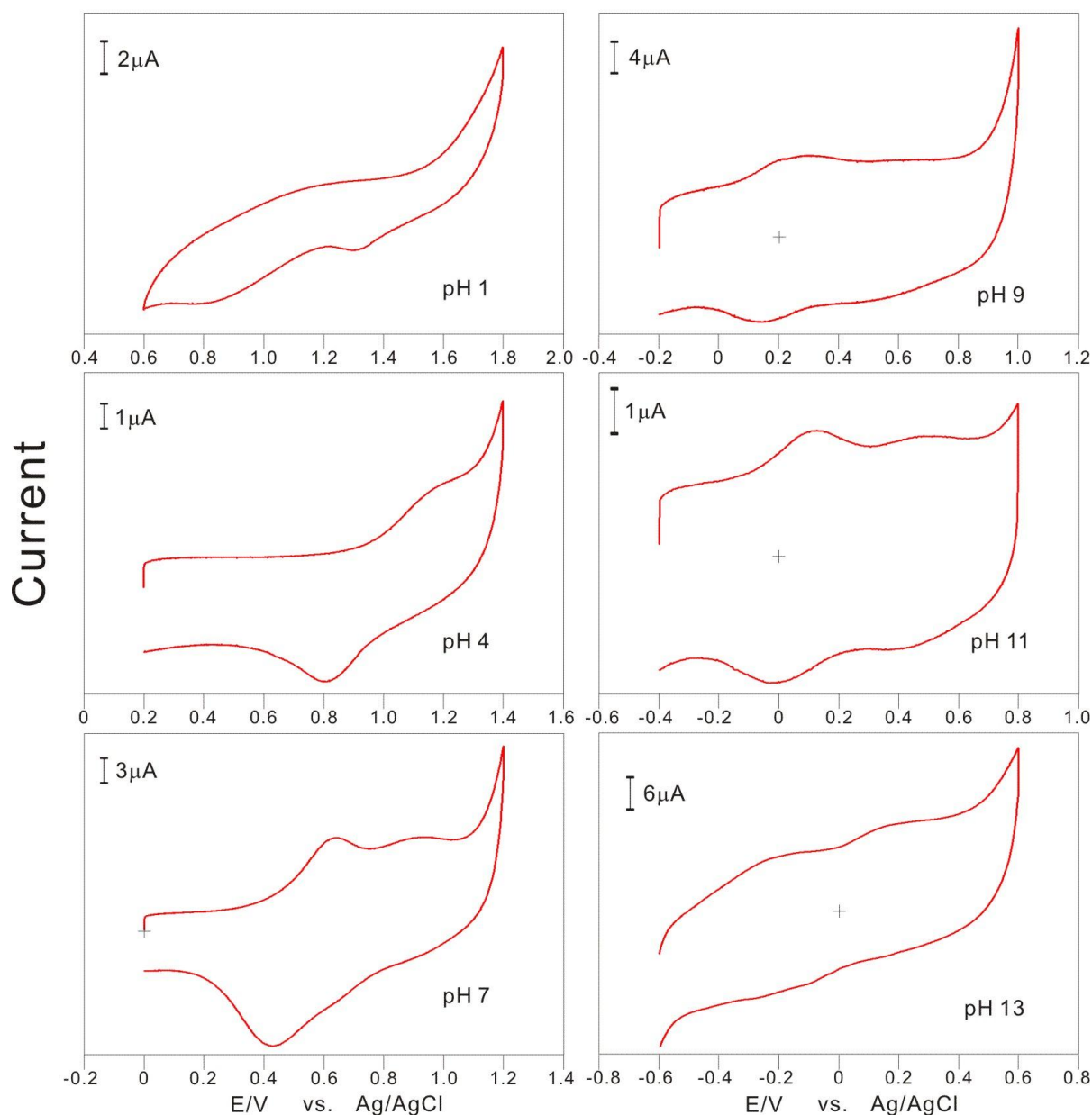


Figure 3. CV response of nano manganese oxide modified ITO in various buffer solutions (pH: 1, 4, 7, 9 and 13)

During the continuous repetitive cycling process, the corresponding anodic and cathodic peak currents increase linearly. This process confirms the electrodeposition of nano manganese oxide at the

ITO surface. Based on the XRD pattern discussion (Fig. 1(C)), the electrodeposited nano manganese oxides were found in different phases. Therefore, the corresponding anodic and cathodic peaks clearly represent the different phases (MnO , MnO_2 and Mn_3O_4) of the electrodeposited manganese oxide nanoparticles. To examine the electrochemical activity, at first, the nano manganese oxide modified ITO examined in pH 7.0 PBS. Here considering the physiological pH conditions for the electrocatalysis, at first we have selected pH 7.0 PBS for the electrocatalytic applications. Figure 2 (B) represents the different scan rate studies of the nano manganese oxide modified ITO in pH 7.0 PBS. From the Fig. 2(B) we can clearly notice that for the increasing scan rates (0.01 to 1 V/s), the corresponding reduction and oxidation peaks increasing clearly with more negative and positive shifts, respectively. Further the Inset of Fig. 2(B) shows the anodic and cathodic peak current (I_p) vs. scan rate (V/s) of the nano manganese oxide modified ITO. Here both the anodic and cathodic peak currents increase in linear manner which shows that the nano manganese oxide is electrochemically active and stable in pH 7.0 PBS.

In the next step, fabricated nano manganese oxide particles have been examined in various buffer solutions (pH 1, 4, 7, 9 and 13). From the Fig. 3 we can see the electrochemical response of the nano manganese oxide modified ITO. In pH 1 solution, the reduction peak appears at the potential of (E_{pc}) 1.3 V. At the same time, in pH 4, the corresponding reduction peak appears at 0.81 V and the anodic peak appears around at 1.15 V. In the pH 7.0 PBS, the anodic and cathodic peak appears at the potential range of 0.62 and 0.91 and 0.43 V. In the pH 9 and 11 solutions, it appears as a broad curve and the corresponding anodic and cathodic peak appears at 0.26 V, 0.14 V and 0.09 V, -0.006 V. Further in pH 13 it shows background current increase with the diminished oxidation and reduction peak currents, respectively. From this results, it shows that the nano manganese oxide particles were electrochemically active in all pH solutions. However, it clearly exhibits the reduction and oxidation peak currents in pH 4, 7, 9 and 11 solutions, respectively. Here the CV curve differs at the various buffer solutions because; the presence of different phases of manganese oxide which exhibits different electrochemical activities in the buffer solutions.

Electrochemical activities of the film modified electrodes could be assessed and clearly illustrated using electrochemical impedance spectroscopic analysis (EIS). In the EIS analysis the complex impedance spectrum of the bare and film modified electrodes presented as a sum of the real Z' (ω) and imaginary Z'' (ω) components that originates mainly based on the resistance and the capacitance behavior of the cell. Based on the shape of the impedance spectrum of both bare and film modified electrodes, the electron-transfer kinetics and diffusion characteristics can be elucidated. These semicircle parameters correspond to the electron transfer resistance (R_{et}) and the double layer capacity (C_{dl}) of the corresponding electrodes. Fig. 4(A) exhibits the Faradaic impedance spectra shown as Nyquist plots (Z'' vs. Z') for the bare (curve b) and nano manganese oxide modified ITO (curve a). Here bare ITO (curve b) exhibits as a big semi circled arc with the (R_{et}) value of 199 ($Z'/K\Omega$). For the nano manganese modified ITO, exhibits with a small semi circled arc with lower (R_{et}) value of 132 ($Z'/K\Omega$). In this regard, the bare ITO holds the higher (R_{et}) value comparing with the modified ITO clearly illustrates that the electron transfer process is more active comparing with the bare ITO. Inset of Fig. 4(A) shows the simple Randles circuit model based on the impedance spectrum of the nano manganese oxide modified ITO. The maximum impedance error for this fit model was

found as 4.8 %. From this EIS discussions we can conclude that the nano manganese oxide modified ITO could be applied for the various types of electrochemical applications.

3.3. Electrocatalytic applications of nano manganese oxide modified ITO

Nano manganese oxide particle modified ITO was employed for the detection of H_2O_2 .

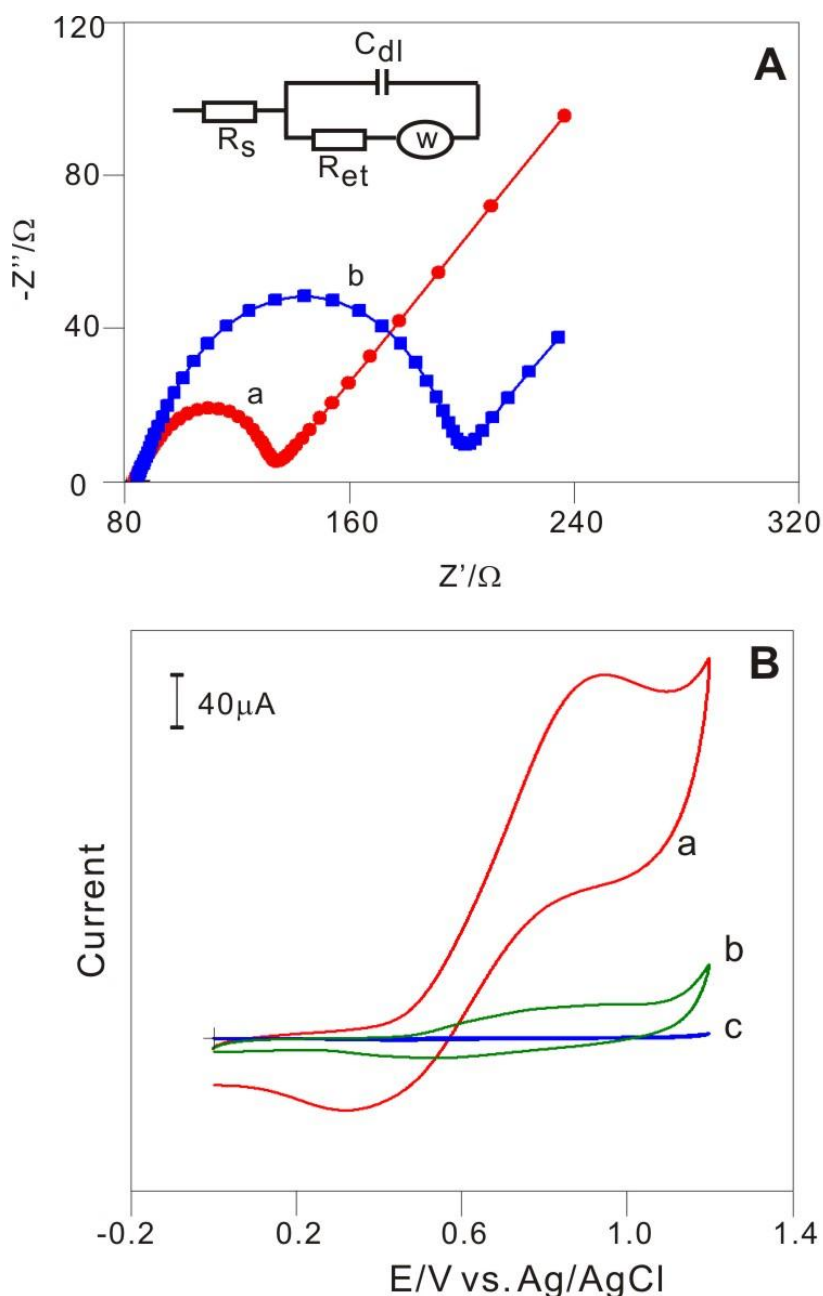


Figure 4. (A) Electrochemical impedance spectra curves of (a) nano manganese oxide modified ITO, (b) bare ITO in pH 7.0 PBS containing 5×10^{-3} M $[\text{Fe}(\text{CN})_6]^{3-/4-}$ (Amplitude: 5 mV). (B) A) CV response of nano manganese oxide modified ITO in (a) pH 7.0 PBS containing 1.91×10^{-3} M H_2O_2 and (b) in pH 7.0 PBS (blank solution). (c) Bare ITO response for the H_2O_2 (1.91×10^{-3} M) in pH 7.0 PBS.

Considering the physiological pH, we have employed pH 7.0 PBS for the electrocatalytic applications. Cyclic voltammetry (CV) and differential pulse voltammetry (CV) were applied for the electrocatalysis. To evaluate the electrocatalytic advantage of the proposed material modified ITO, it has been compared with bare ITO. Fig. 4(B) shows the CV response of bare (curve c), nanomanganese oxide modified ITO (curve a) for the H_2O_2 electro oxidation process.

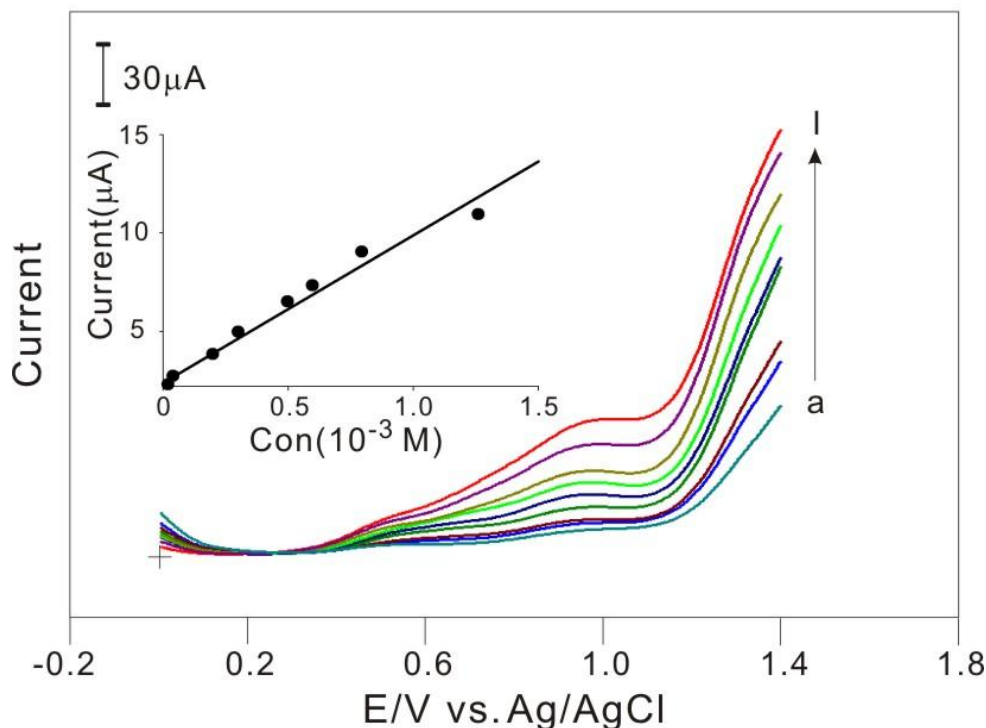


Figure 5. DPVs for the detection of H_2O_2 at the nano manganese oxide modified ITO in pH 7.0 PBS. H_2O_2 concentrations were in the range of (a-I): 0, 0.02, 0.04, 0.2, 0.3, 0.5, 0.6, 0.8 and 1.26 mM. Inset shows the calibration plot of current vs. concentration plots of H_2O_2 .

The proposed nanomaterials modified ITO shows enhanced current response for the detection of H_2O_2 (0.86 V) (curve a). At the same time the bare ITO shows only the diminished current response for the detection of H_2O_2 . According to this result, it shows the nano manganese oxide modified ITO is suitable for the detection of H_2O_2 .

Generally, pulse voltammetry gives better results and sensitivity than CV. Therefore, here we have employed DPV for the electrocatalytic detection of H_2O_2 . Fig. 5 exhibits the DPV response of nano manganese oxide modified ITO for the electrocatalytic oxidation of H_2O_2 . For the frequent additions of H_2O_2 , the nano manganese oxide clearly shows the anodic current response for the detection H_2O_2 . It shows the anodic current response for the H_2O_2 detection in the linear range of 0.02 to 1.26 mM. Further the sensitivity and the detection limit of this electrode for the detection of H_2O_2 was found as $7.513 \mu\text{A mM}^{-1}$ and 0.02 mM.

In the next step, H_2O_2 containing antiseptic solutions were examined for the real sample analysis. Fig. 6 exhibits the DPVs of nanomanganese oxide modified ITO for the detection of H_2O_2 .

For the 0.02 to 1.26 mM concentration range the proposed nanomaterials clearly shows the anodic current response for the detection of H_2O_2 . Here, the anodic peaks appear at 0.53 and 0.91 V. Based on the Fig. 4 (A) results, we consider that the anodic peak at 0.91 V corresponds to the electrooxidation of H_2O_2 . According to the above discussions, we can conclude that the nano manganese oxide modified ITO holds the capacity for the detection and determination of H_2O_2 both in lab and real samples, respectively.

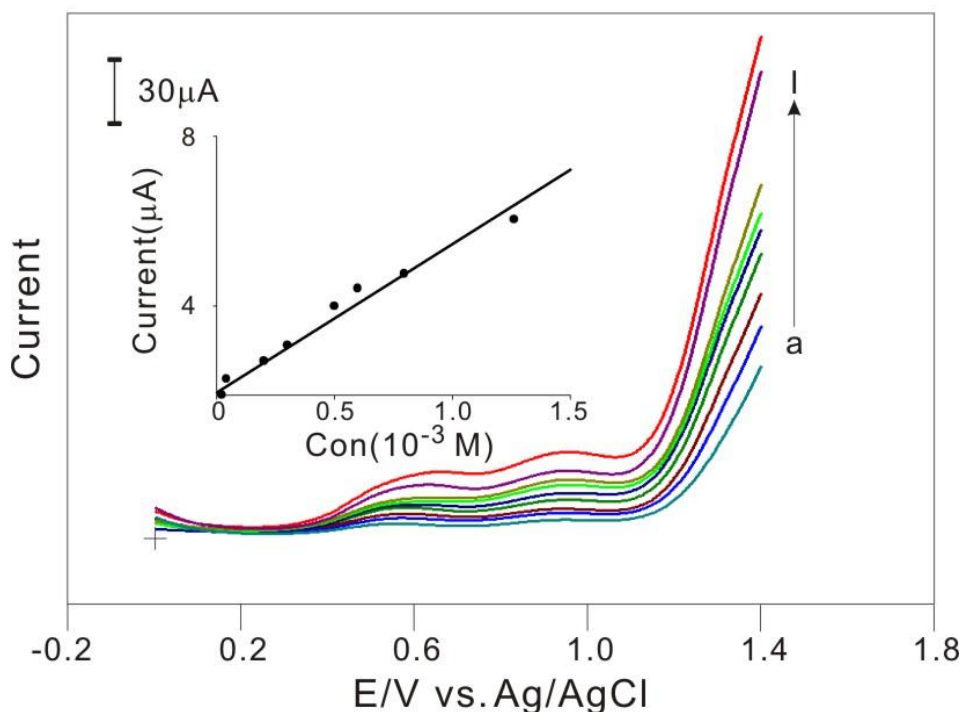


Figure 6. DPVs for the detection of H_2O_2 (in real sample) at the nano manganese oxide modified ITO in pH 7.0 PBS. H_2O_2 concentrations were in the range of (a-I): 0, 0.02, 0.04, 0.2, 0.3, 0.5, 0.6, 0.8 and 1.26 mM. Inset shows the calibration plot of current vs. concentration plots of H_2O_2 (in real sample).

4. CONCLUSION

Nano manganese oxide particles were successfully electrodeposited on ITO using cyclic voltammetry. Fabricated nano manganese oxide particles were found as electrochemically stable and active in various pH conditions. Proposed nanomaterials modified ITO holds the capacity for the electrochemical detection and determination of H_2O_2 in lab and real samples in the appropriate linear ranges with good detection limit and sensitivity. Finally, this type of nanomaterials modified ITO could be employed for the fabrication of H_2O_2 sensor applications.

ACKNOWLEDGMENT

This work was supported by grants from National Science Council (NSC) of Taiwan (ROC).

References

1. F. Torres, R. Amigo', J. Asenjo, E. Krotenko, J. Tejada, *Chem. Mater.*, 12 (2000) 3060.
2. Y. Yang, L. Xiao, Y. Zhao, F. Wang, *Int. J. Electrochem. Sci.*, 3 (2008) 67.
3. C.-Y. Cheng, S. Thiagarajan, S.-M. Chen, *Int. J. Electrochem. Sci.*, 6 (2011) 1331.
4. A. Dierstein, H. Natter, F. Meyer, H.-O. S.C. Kropf, R. Hempelmann, *Scripta Mater.*, 44 (2001) 2209.
5. L. Espinal, S.L. Suib, J. F. Rusling, *J. Am. Chem. Soc.*, 126 (2004) 7676.
6. M.S. El-Deab, T. Ohsaka, *J. Electrochem Soc.*, 153 (2006) A1365.
7. S.C. Pang, S.F. Chin, Y.Y. Tay, C. L. Tay, *ICONN* 06, 3-7 (2006), doi: 10.1109/ICONN.2006.340539.
8. H. Adelkhani, M. Ghaemi, M. Ruzbehani, *Int. J. Electrochem. Sci.*, 6 (2011) 123.
9. M.S. El-Deab, T. Ohsaka, *Electrochim Acta* 52 (2007) 2166.
10. I. Roche, E. Chai'net, M. Chatenet, J. Vondra'k, *J. Phys. Chem. C* 111 (2007) 1434.
11. D. Zhang, D. Chi, T. Okajima, T. Ohsaka, *Electrochim Acta* 52 (2007) 5400.
12. K.Q. Ding, *Int. J. Electrochem. Sci.*, 5 (2010) 72.
13. S. Chen, J. Zhu, X. Wu, Q. Han, X. Wang, *ACS Nano*, 4 (2010) 2822.
14. R.K. Sharma, A.C. Rastogi, S.B. Desu, *Electrochim Acta* 53 (2008) 7690.
15. F.-J. Liu, T.-F. Hsu, C.-H. Yang, *J Power Sources* 191 (2009) 678.
16. R. Liu, J. Duay, S.B. Lee, *Acs Nano* 4 (2010) 4299.
17. M.S. El-Deab, M.I. Awad, A.M. Mohammad, T. Ohsaka, *Electrochem Commun.*, 9 (2007) 2082.
18. M.S. El-Deab, *Int. J. Electrochem. Sci.*, 4 (2009) 1329.
19. P. Norouzi, F. Faridbod, E.N. Esfahani, B. Larijani, M. R. Ganjali, *Int. J. Electrochem. Sci.*, 5 (2010) 1008.
20. F. Cheng, Y. Su, J. Liang, Z. Tao, *J. Chen, Chem. Mater.*, 22 (2010) 898.
21. Y. Usui, K. Sato, M. Tanaka, *Angew. Chem.*, 42 (2003) 5623.
22. E.A. Mazzi, K.F.A. Soliman, *J. Appl. Toxicol.*, 24 (2004) 99.
23. P.A. Tanner, A.Y.S. Wong, *Anal. Chim. Acta* 370 (1998) 279.
24. N.V. Klassen, D. Marchington, H.C.E. McGovan, *Anal. Chem.*, 66 (1994) 2921.
25. O.S. Wolfbeis, A. Durkop, M. Wu, Z. Lin *Angew. Chem. Int. Ed.*, 41 (2002) 4495.
26. X. Shu, Y. Chen, H. Yuan, S. Gao, D. Xiao, *Anal. Chem.*, 79 (2007) 3695.
27. Y. Lvov, B. Munge, O. Giraldo, I. Ichinose, S. Suib, J.F. Rusling, *Langmuir* 16 (2000) 8850.
28. G. Zhao, J.J. Xu, H.Y. Chen, *Electrochem. Commun.*, 8 (2006) 148.
29. A. Salimi, R. Hallaj, S. Soltanian, H. Mamkhezria, *Anal. Chim. Acta* 594 (2007) 24.
30. A. Salimi, E. Sharifi, A. Noorbakhask, S. Soltanian, *Electrochem. Commun.* 8 (2006) 1499.
31. G. Zhao, J.J. Feng, J.J. Xu, H.Y. Chen, *Electrochem. Commun.* 7 (2005) 724.
32. J.J. Feng, J.J. Xu, H.Y. Chen, *Electrochem. Commun.*, 8 (2005) 77.
33. Y. Li, J. Zhang, H. Zhu, F. Yang, X. Yang, *Electrochim Acta* 55 (2010) 5123.
34. L. Zhang, Z. Fang, Y. Ni, G. Zhao, *Int. J. Electrochem. Sci.*, 4 (2009) 407.
35. C.-K. Lin, K.-H. Chuang, C.-Y. Lin, C.-Y. Tsay, C.-Y. Chen, *Surf. Coat. Tech.*, 202 (2007) 1272.
36. C.-Y. Chen, C.-K. Lin, M.-H. Tsai, C.-Y. Tsay, P.-Y. Lee, G.-S. Chen, *Ceram. Int.*, 34 (2008) 1661.
37. G. Anoop, K. M. Krishna, M.K. Jayaraj, *Appl. Phys. A* 90 (2008) 711.
38. L. Chen, Y. Shen, J. Bai, *Mater. Lett.*, 63 (2009) 1099.